Completion and operational testing of the Adams' permanent magnet electric D.C. motor-generator

Conference Paper · May 2015

DOI: 10.1109/EPE.2015.7161173

2 authors, including:

Petr Kacor
VŠB-Technical University of Ostrava
37 PUBLICATIONS **79** CITATIONS

SEE PROFILE

Completion and Operational Testing of the Adams' Permanent Magnet Electric D.C. Motor-Generator

Martin Koutný, Petr Kačor
VŠB - Technical University of Ostrava
Department of Electrical Power Engineering
Ostrava – Poruba, Czech Republic
martin.koutny.st3@vsb.cz, petr.kacor@vsb.cz

***Abstract*—This paper focuses on description of the operation principle inherent to the Adams' electric motor-generator fitted with permanent magnets made of rare earth (NdFeB). There is a certain part dedicated to distribution of the magnetic field within the magnetic circuit of rotor and stator monitoring by means of the Ansys Workbench software. The Adams' motor generator is basically assembled with slight deviations from the original patent with respect to the stator magnetic circuit design. The resultant speed-torque characteristics obtained by measurement and the input power values have been processed to determine the machine's efficiency.**

Keywords—Adams motor-generator*; *electric motor-generator*; *Ansys*; *permanent magnet*; *NdFeB*; *efficiency*; *zero point energy*; *non-conventional electric machinery

I. INTRODUCTION

The electric machinery field has not has any major advances in development since Nikola Tesla made his first successful inventions. Nevertheless, there are still numerous sources of instructions and patents for electric machinery published online; their authors even claim this equipment would work at efficiency levels exceeding the 100% mark. More precisely, if any of these machines were really functioning, it would have to be supplied with some kind of energy from the outside to undergo transformation into a directly usable form of energy. That happens in heat pumps, for example. This is not about efficiency yet rather the efficiency factor COP>1 in this respect. That is actually the ratio of power coming into the system from the ambient environment and the power used for control of the system. The said process is illustrated by the block diagram in Fig. 1.

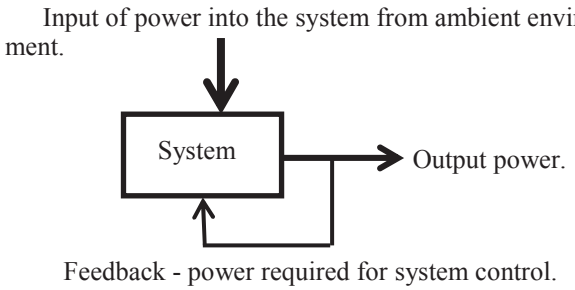

Fig. 1. Process for utilisation of power from the ambient environment.

The emerging hazard represented by the lack of main power source fuels in form of coal and natural gas is defined in the Hubbert Peak Theory, for example, also known as the "peak oil". [1]

When searching for power sources that may be able to outrank the ones currently used in many aspects, one may encounter the term "Zero point energy (ZPE)". [2]

ZPE is apparently indicated by electromagnetic fluctuations in vacuum, which is also at 0 K theoretically. [3]

There are numerous printed materials dealing with existence of ZPE and events associated with it. [3], [4].

One of the phenomenons to be mentioned is the space-filling high-frequency electromagnetic noise. [5]

The nature of ZPE has initiated implementation of the so-called "virtual particles". [2]

The occurrence can be proven by the so-called "Casimir effect", for example. [6]

The question is, whether, how and to what extent this source can be utilised as far as the volume of usable energy is concerned. One of the literary resources addressing this issue is the [9].

II. OPERATION OF THE ADAMS' MOTOR-GENERATOR IN DETAIL

Fig. 2. (a) is the pole of rotor R1 right in between the stator poles S1 and S2.

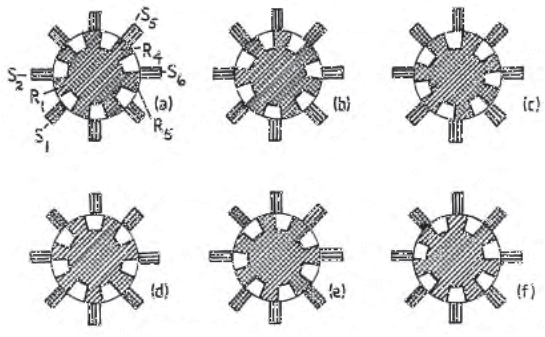

Fig. 2. Mutual positions of rotor and stator poles during rotation of the rotor.

Work was partially supported by SGS grant VŠB-TU Ostrava No. SP2015/192.

978-1-4673-6788-2/15/$31.00©2015 IEEE

Imagine that it inclines towards S2, being attracted to the latter until setting at the position indicated in Fig. 2. (c). It is aligned with the stator core now, current beginning to pass through its coils with such polarity to induce repulsion of the rotor pole from the position with aligned axes of the rotor salient pole and the stator core. It is therefore accelerated pursuant to strong interaction of magnetic fields of the rotor. The current will keep entering the stator coils until the stator has reached the position shown in Fig. 2. (e). The opposite stator core will be aligned with the rotor salient pole now.

Let us look what happens on the opposite side of the rotor during this process.

Rotor pole R4 in Fig. 2. (a) is currently aligned with the stator core S5. That is why the winding in core S5 is supplied with electric current the effects of which induce potential repulsion of the pole R4. The current is passing through winding of the core S5 till the moment illustrated by the Fig. 2. (c), when the core of stator S2 is de-magnetised.

The rotor is spun by the following force contributions:

a) The rotor pole is attracted to the magnetic stator cores by magnetic forces produced by permanent magnets protruding into the air gap and closed over the stator cores.

b) Once aligned with the rotor salient pole, the rotor is further spun by repulsive forces between rotor poles and the stator core. Coils in stator cores are supplied with electric pulses depending on the position of rotor with respect to the stator. The magnetic field within the air gap will reach its maximum intensity once the poles of both rotor and stator have been aligned.

III. Completion of Non-Conventional Adams' Electric Motor-Generator

My choice for operational testing focused on Adams' electric D.C. motor-generator with permanent magnets inside its rotor. The description of motor-generator provided by Robert George Adams from new Zealand and Harold Aspen from the United Kingdom talks about its ability to draw ZPE through the air gap between magnetic poles of the rotor and stator. [8]

R. Adams has compiled his manual for a test sample of this machine to calculate its efficiency using the ratio of power on the supply lead battery for commissioning of the machine and voltage of the battery being charged at the machine output side. [7] However, the efficiency figure obtained from this calculation does not consider any power consumed by mechanical work of the rotor, the charging characteristics of the lead battery employed and the efficient of the re-charging process itself. That is why the resultant efficiency figure is distorted by these factors. The machine described in this paper still differs from the original patent in some aspects that may have a significant impact on its resultant efficiency. The main difference lies in shapes of magnetic stator cores.

A. Machine Magnetic Circuit Analysis

The right side of Fig. 3. shows the lateral view of one core in the stator and the rotor salient poles with the permanent rotor magnet highlighted in yellow, this colour corresponds to the value of approximately 1.1 T. The greatest induction values are evident in the stator core shoulder. The vertical line of induction values (in the centre of this figure) describe the air gap.

For illustration of the magnetic induction using a vector, see Fig. 4. that clearly shows the induction curves forming closed paths evidenced by the third Maxwell's equation.

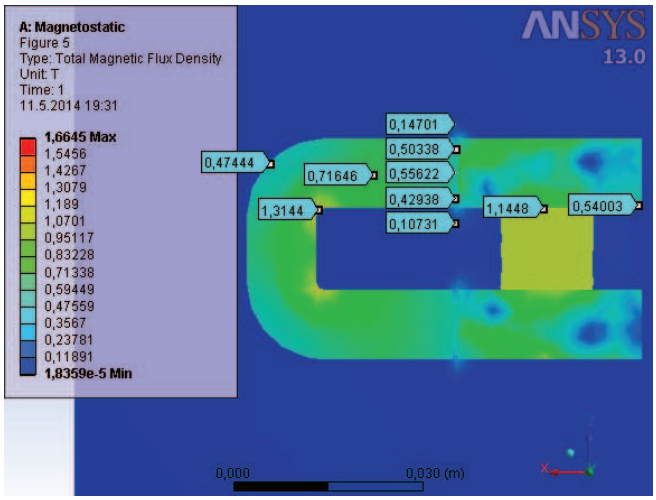

Fig. 3. View of the magnetic induction distribution within magnetic field of circuits in the rotor (right) and the stator (left) at the zero point energy (not shown).

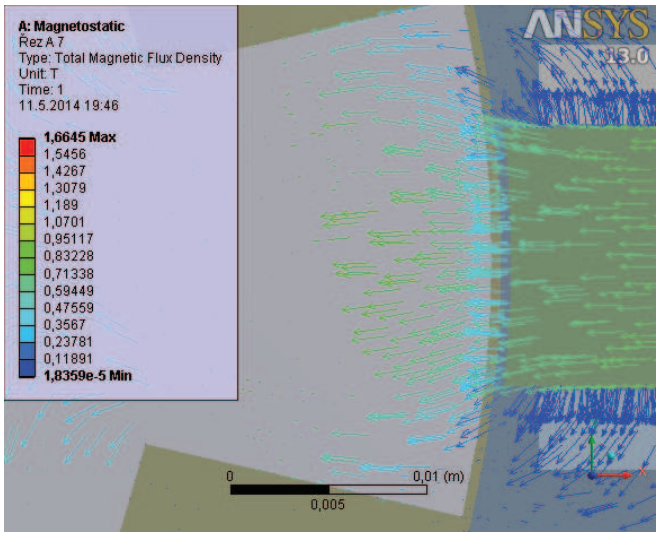

Fig. 4. Top view of the magnetic vector distribution inside magnetic circuits of the rotor (left) and the stator with zero current passing through coils.

B. Machine Electronic Section

The machine was initially connected as a motor benefiting from the wiring shown in the Fig. 5. The performance section is actuated upon interruption of an infrared beam landing on the phototransistor in the optocoupler. The beam passes through the transparent foil part at the moment, when the rotor salient poles are in the front position together with stator cores with the magnetic induction flow initiated by coils; this flow is opposite to the power flow coming out of the rotor poles. The rotor is spun by forces acting between magnetic fields of the rotor and the stator.

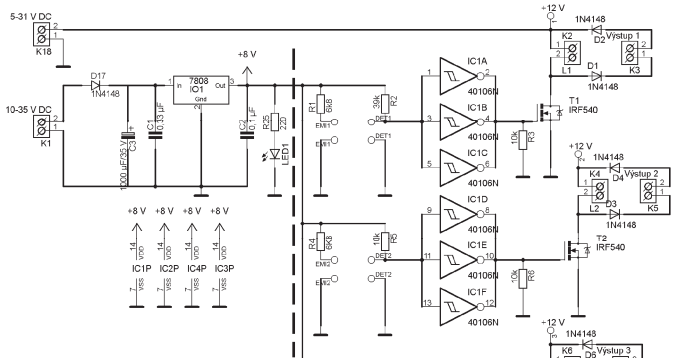

Fig. 5. Wiring diagram of the electric circuit for motor control. The circuit in the right side of the figures behind dashed line is repeated 4 times in total. The figure shows one quarter of the wiring only to save space.

The electric circuit can be divided into the output part separated from the low input power section by means of a control electrode MOSFET on IRF540N transistors. The left side of this diagram shows the connection points of supply voltage. The positive pole of 5-31 V direct current supply voltage is linked with stator coils via connectors L1 to L8. The voltage of 10 – 35 V DC is connected via the voltage regulator 7808. This diagram shows the optocoupler TCST 2103 represented by outlets marked EM1 and DET1. The resistance values are determined in order to limit the current in control circuit to the lowest value, while preserving correct operation of the circuit. The beam passes through transparent part of the commutator, as it is interrupted by the piece printed with black colour. Schmitt trigger circuits are connected behind detectors to invert the voltage at the input point. One enclosure of the integrated circuit 40106 includes 6 investing gates. The parallel connection of three gates in each batch helps reduce the gate resistance to one third of its initial value. That is followed by the N-MOSFET type output IRF560N transistor with low-resistance electrode transition DS in actuated state equal to 44 mΩ. Once the transistor opens, the current will be passing through the relevant winding linked with the connector. Connection of contacts K3 ensures engagement of the transistor overvoltage protection in terms of serial connection of rectifier diodes D1 and D2.

The patent claim of Robert Adams describes coils connected in series and situated on mutually opposite magnetic cores of the stator. Fig. 6. shows one of the possible configurations of the machine indicating serial connections of coils situated mutually opposite.

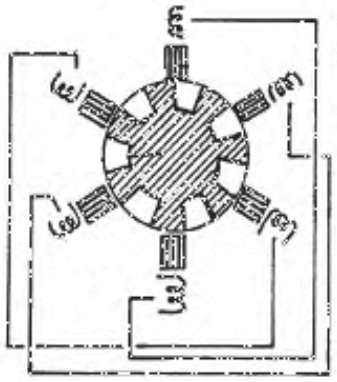

Fig. 6. Machine configuration with 6 stator poles and 7 rotor poles. Magnetising winding of opposite poles of the stator are connected in series.

According to the patent author, the connection shown in Fig. 6. enables this machine to connect the motor and generator functions within, provided it has been spun to a certain speed using an external motor that is subsequently disengaged, for automatic generation of torque or electric power on the shaft. It may be drawn from the auxiliary coils in the stator (not shown) from any couple of drive stator coils or a conventional generator connected with the shaft of Adams' motor-generator.

IV. Practical Implementation of Adams' Motor-Generator

Fig. 7. shows the front view of the implemented machine. When working as an electric motor, the machine is supplied with direct current impulses depending on the position of the rotor salient poles with respect to the stator poles. The ratio between rotor and stator poles is 7:8. This ratio always helps the rotating rotor align axes of rotor poles and stator cores at a single salient pole of the rotor and one magnetic core of the stator. The axis of stator core is situated in the middle of the gap between the rotor salient poles on the opposite side.

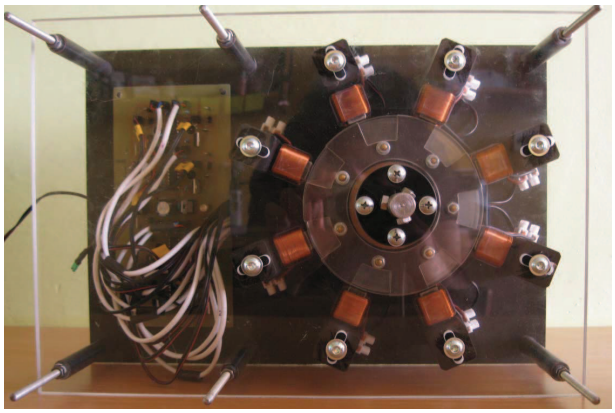

Fig. 7. Front view of the finished model of the implemented Adams' motor-generator.

A. Rotor

The rotor is fitted with 7 permanent magnets NdFeB with magnetisation rating of N38 and 15 mm in diameter and 13 mm in height. These magnets are situated between two sections made of stratified metal laminations made of steel M600-50. These laminations are cut with a water jet into a gear shape with alternating 7 gaps and 7 teeth forming salient poles supported by magnetising of magnets. The Fig. 8. shows an assembled rotor.

B. Stator

Foundation for the rigid stator structure is made of two 8 mm thick perspex pads fitted with ball bearings and wooden holders for attachment of magnetic cores of the stator containing the cores glued in with epoxy resin. The magnetic circuit of stator comprises 8 soft C-shaped magnetic cores coiled from the material M150-30 S and provided with a pair of excitation coils connected in series. The cores are spaced evenly around the rotor circumference and they were originally designed for core-type transformers.

Fig. 8. View of a rotor comprising a shaft, fixing flanges, a magnet enclosure, rotor sections and stratified laminations and side perspex panels with brass bolts to tighten the rotor body

C. Commutator

Fig. 9. Shows the commutator comprises a transparent foil printed with a pattern of alternating black and transparent spots. When the optocoupler beam passes through the transparent foil, electric current supply will be actuated for the relevant pair of coils on one of the eight stator cores. Location of eight optocouplers around the circumference of the black commutating foil is evident from Fig. 9. The foil can be tilted within the range between -12.85° and 12.85° with respect to its default position to achieve the optimal moment of current switching for the relevant coils.

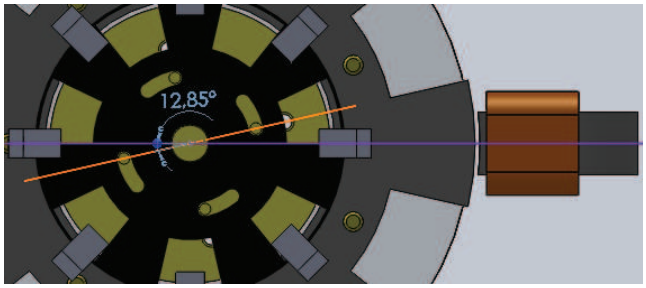

Fig. 9. Setting the lead angle of commutating foil to -12.85° with respect to the default position.

D. Difference from Original Patent

The configuration of implemented machine is shown in Fig. 10. and it differs from the original patents by the shape of stator cores. The author makes use of soft magnetic cores of block shape. The implemented machine makes use of C-shaped oriented cores due to lack of block-shaped cores of the desired material M150-30S.

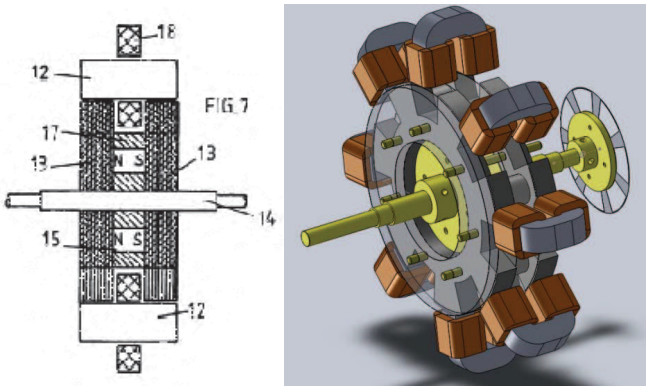

Fig. 10. Structural view of the rotor from original patent (left). View of the rotor with stator cores fitted with coils connected in series (brown) and the commutating foil attached to the machine shaft (right).

V. Electric Measurements on Machine

Time paths of voltage and current shown in the Fig. 11. have been measured on one of the eight stator coils at the voltage level of 30V and under the mechanical load of Mz = 0.15 Nm. The paths were measured using a professional two-channel USB oscilloscope Handyscope HS3.

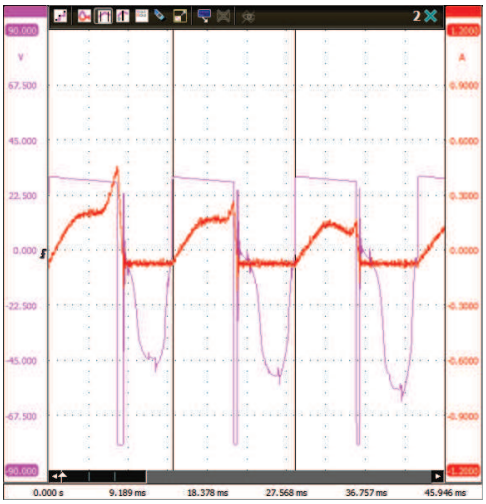

Fig. 11. Measured paths of voltage and current on stator coils when subject to the torque load of 0.15 Nm.

The average resistance of the coil pairs connected in series inside the stator core is 20.34 Ω.

Fig. 11. shows a high-voltage peak with opposite polarity with respect to the supply voltage, reaching the value of -79.96 V. That occurs due to sudden interruption of power supply into the coil circuit. The magnetic field created within the magnetic circuit attempts to prevent its changes after an interruption of the initiating power supply and keeps current within the electric circuit to induce high voltage with reversed polarity back to the electric circuit. This event is expressed by the second Maxwell's equation dealing with the magnetic induction rule in differential form defined by the formula (2). [10]

$$\nabla \times \mathbf{E} = -\frac{\partial \mathbf{B}}{\partial t} \tag{2}$$

Fig. 11. shows the evident endurance range at the end of the negative voltage peak. This endurance range is caused by the parasitic coil capacity. The time constant of the event fading is determined by RLC parameters of the circuit.

A. Measurement of Essential Characteristics of the Machine

Fig. 12. shows a diagram of the load cell and motor for measurement of the motor torque characteristics at various rotation angles of the commutating foil.

The machine served as a motor with separately excited load cell. The option for control of reaction torque by change in resistance of the load cell armature and the magnitude of the excitation current enabled measurement of the course of speed-torque characteristic. Linkage of the shaft and a speed-voltage generator enabled measurement of voltage induced during individual measurements to calculate the relevant speed.

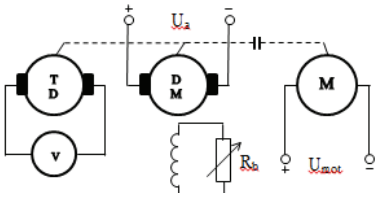

Fig. 12. Assembly for measurement of the motor load characteristics comprising the speed-voltage generator (TD) for measurement of speed, the separately excited load cell (DM) and the machine implemented as motor (M). Where: Ua – load cell armature voltage (V), Rb – variable resistor within the separate excitation circuit (Ω), Umot – supply voltage to the machine operated as motor (V).

Fig. 13. shows a speed-torque characteristic of the machine operated as motor for rotation of the commutating foil to said angles.

Fig. 14. shows a Dependence between the motor efficiency and mechanical output, for individual rotation angles of the commutating foil.

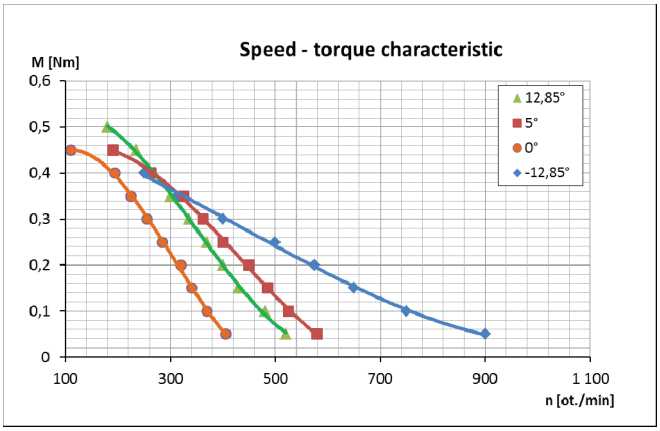

Fig. 13. Speed-torque characteristic of the machine operated as motor for rotation of the commutating foil to said angles.

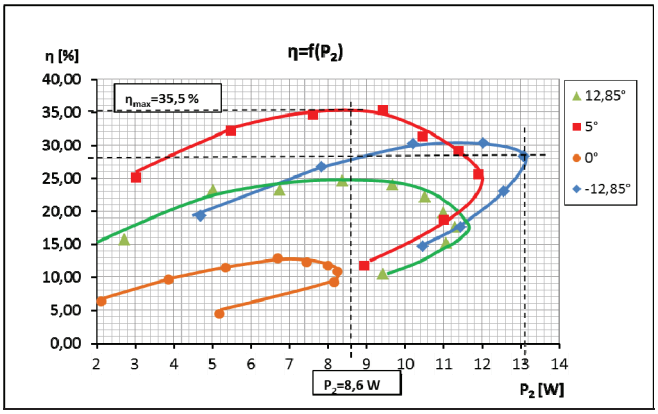

Fig. 14. Dependence between the motor efficiency and mechanical output, for individual rotation angles of the commutating foil.

B. *Efficiency of Machine Operated as Motor*

The example of efficiency calculation was based on the existing formulas supplied with values of quantities corresponding with the maximum motor efficiency.

As the current flowing into coils is direct, the input power of the motor will be determined as a product of the constant supply voltage of 31 V and the current flowing

$$P_1 = U \cdot I \tag{3}$$

through

$$P_1 = 31 \cdot 0{,}86 = \underline{26{,}66\ W} \tag{4}$$

the circuit. The input power is defined by the formula (3)

$$\omega = 2\pi \frac{n}{60} \tag{5}$$

Entering the maximum speed will produce the rotor circular orbit speed

$$\omega = 2\pi \frac{450}{60} = \underline{47{,}12\ rad^{-1}} \tag{6}$$

The circular orbit speed expressed by means of speed

Entering of the angular speed values produces the resul-

$$P_2 = M \cdot \omega \tag{7}$$

tant output on the machine shaft

The motor efficiency is equal to the product of torque

$$P_2 = 0{,}2 \cdot 47{,}12 = \underline{9{,}42\ W} \tag{8}$$

produced and the circular orbit speed

Entering of the angular speed values produces the resultant output on the machine shaft

The motor efficiency, excluding the negligible losses inside the electric circuit, is determined by the ratio of output and input power

The resultant efficiency of the implemented machine, with optimal timing for switching of current into coils after enter-

$$\eta = \frac{P_2}{P_1} \cdot 100 \tag{9}$$

ing of the relevant values, is equal to (10).

$$\eta = \frac{9{,}42}{26{,}66} \cdot 100 = \underline{\underline{35{,}33\ \%}} \tag{10}$$

C. *Characteristic of Machine Implemented as Motor-Generator*

Linkage of shafts of the implemented machine with a direct-current motor will enable us to use such assembly to drive the machine implemented as motor-generator. If the implemented machine showed characteristics stated by the author of patent, it should prove its self-supplying ability once it has reached a certain speed level. That would reduce the current in armature of the driving direct-current motor.

There were two measurements performed to enable comparison of change in reaction torque expressed as a change to the current in armature of the direct-current motor. The first measurement was conducted with coils on opposite stator cores disengaged; those were connected in series during the second measurement.

The measurement was performed under constant excitation of the direct-current motor using the voltage U_b=2.2 V (I_b=1.16A).

The armature voltage on direct-current motor was controlled to achieve a speed change of assembly. The magnitude of current induced within the circuit with opposite coils of stator cores connected in series had no significant impact on the path of current increase within the armature perimeter when the speed rises. The paths of current increase in the armature I_a for both cases, depending on the controlled increasing armature voltage Ua on the direct-current motor, are shown in the Fig. 15.

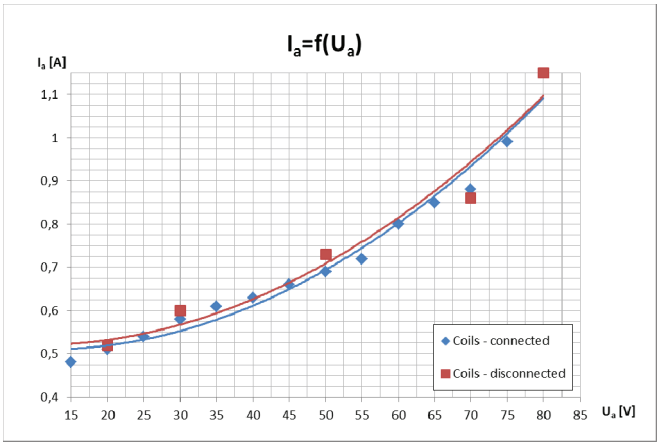

Fig. 15. Comparison of paths of the current in armature of the direct-current motor, depending on the change of armature supply voltage for connected and disconnected opposite stator coils.

VI. Conclusion

The patent author, Robert Adams, determined the efficiency of his motor-generator using a five-day long measurement. He measured paths of voltage on the input battery powering the machine, together with the voltage on batteries being connected to the electric output of the machine in progressive order. The machine in operation also re-charged the output batteries. The voltage values obtained by measurement during continuous measurement are certainly an indicator of machine efficiency, yet the calculation of accurate efficiency defined by the ratio of output and input power would require inclusion of currents passing through the circuit.

As the magnetic stator cores differ in shape, one cannot surely consider the Adams' motor generator described by the author as unable to draw ZPE.

The maximum efficiency measured on the implemented machine operated in motor mode has been set to 35.33 %. Owing to the significant dispersion of magnetic flow beyond effective routes within the magnetic circuit, the efficiency value is appropriate and compliant with the classic theory on electromagnetic fields. According to the patent author, the machine working as motor-generator is able to continue with independent operation without any evident external supply of voltage once commissioned by means of a separate motor. This condition has not occurred, as evidenced by the Fig. 15. Verification of the described self-charging function shall be addressed during future activities seeking non-conventional environment-friendly sources of electric power.

References

[1] M. King Hubbert, “Nuclear energy and the fossil fuels”, 1956, No. http://www.hubbertpeak.com/hubbert/1956/1956.pdf

[2] T. Valone, “Zero Point Energy: The Fuel of the Future,” United States: Integrity Research Institute, 2007, 228 s. ISBN 9780964107021.

[3] B. King Moray, “Quest for Zero Point Energy: Engineering Principles for Free Energy: Engineering Principles for Free Energy,” United States: Integrity Research Institute, 2001, 224 s. ISBN 9780932813947.

[4] H. Kragh, “Archive for History of Exact Sciences,” May 2012, Vol. 66 Issue 3, p199-240. 42p. DOI: 10.1007/s00407-011-0092-3., Academic Search Complete

[5] J. Rafelsky, B. Müller, “The structured vaccum: Thinking about nothing,” Published electrically, 2006. ISBN 3-97144-889-3.

[6] Cornell University Library: arXiv.org [online, cit. 2014-05-08]. http://arxiv.org/pdf/1011.5219v1.pdf

[7] R. George Adams, “ The Adams pulsed motor generator manual,” 46 Landing Roat, Whakanate, Nex Zealand: Nexus magazine, 1992.

[8] R. George Adams, H. Aspen, “Electrical motor-generator,” Patent, GB2282708. 1993.

[9] T. Bearden, “By John Bedini and T.E. Free energy generation: circuits,” 2nd ed. Santa Barbara, Calif.: Cheniere Press, 2006, 806 s. ISBN 09-725-1468-6.

[10] D.Mayer , J. Polák, “Metody řešení elektrických a magnetických polí: vysokoškolská učebnice pro elektrotechnické fakulty,” Praha: SNTL, 1983, 450